Journal of Molecular Catalysis A: Chemical 339 (2011) 92–98

Contents lists available at ScienceDirect

Journal of Molecular Catalysis A: Chemical

journal homepage: www.elsevier.com/locate/molcata

Combustion synthesis, characterization and catalytic application of MoO_3–ZrO_2 nanocomposite oxide towards one pot synthesis of octahydroquinazolinones

Satish Samantaray, B.G. Mishra*

Department of Chemistry, National Institute of Technology, NIT, Rourkela-8, Rourkela, Orissa 769008, India

ARTICLE INFO

Article history:
Received 22 January 2011
Received in revised form 23 February 2011
Accepted 23 February 2011
Available online 2 March 2011

Keywords:
MoO_3–ZrO_2
TEM
UV–vis
Fourier analysis
Octahydroquinazolinones
Combustion synthesis

ABSTRACT

Pure ZrO_2 and MoO_3 (10 mol%)-ZrO_2 nanocomposite oxides were prepared by solution combustion method using glycine as fuel. The synthesized materials were characterized by X-ray diffraction (XRD), Scanning Electron microscopy (SEM), Transmission electron microscopy (TEM) and UV–vis spectroscopic technique. XRD study revealed selective stabilization of the tetragonal phase of zirconia in presence of MoO_3. The crystallite size was calculated from the Fourier line shape analysis of the broadened X-ray diffraction profiles as well as from TEM measurements. Oxide nanoparticles with size in the range of 5–40 nm was observed depending upon the fuel content in the combustion mixture. UV–vis study indicated well dispersion of the molybdenum oxide component in the zirconia matrix in the form of isolated and cluster molybdates. The MoO_3–ZrO_2 nanocomposite oxide was used as an efficient and environmentally benign catalyst for the synthesis of octahydroquinazolinones by multicomponent condensation reaction of dimedone, urea and arylaldehydes in aqueous media as well as under solvent free condition using microwave irradiation. A series of zirconia based heterogeneous catalyst with different acidity and surface area were screened for this reaction. The MoO_3 (10 mol%)-ZrO_2 catalyst was found to be highly active for the transformation with excellent yield and purity of the product in a short reaction time.

1. Introduction

In recent years, considerable attention has been focused on octahydroquinazolinone derivatives because of their potential antibacterial activity against *Staphylococcus aureus*, *Escherichia coli*, *Pseudomonas aeruginosa* and as calcium antagonist [1,2]. The octahydroquinazolinones are synthesized by the multi-component Biginelli reaction route involving one pot condensation of cyclic β-diketones, aromatic aldehydes and urea. Various homogeneous and heterogeneous catalytic systems used for synthesis of octahydroquinazolinone and its derivatives include concentrated HCl in ethanol [2], ionic liquid [3], Nafion-H [4], concentrated H_2SO_4 [5] and TMSCl [6]. Main disadvantages of the reported processes are low yield of products, longer reaction time, use of strongly acidic conditions, formation of side products and handling and recycling of the catalyst. In recent years, enlarging attention on environmental damage and economic factor leads for the development of eco-friendly technology and economic processes. Hence, the synthesis of octahydroquinazolinone derivatives by the Biginelli reaction using solid acid catalysts which are stable, recyclable and environment friendly is highly desirable. Recently, Shingare et al. reported the synthesis of octahydroquinazolinone derivatives using ammonium metavanadate under microwave-irradiation and solvent-free conditions [7]. Herein, we have developed methodology for the synthesis of structurally diverse octahydroquinazolinone using combustion synthesized MoO_3 (10 mol%)-ZrO_2 composite oxides as an efficient and recyclable catalyst under solvent free condition as well as using water as a green reaction media.

Molybdenum oxide is a promising material used in many heterogeneous catalytic processes because of its strong surface acidic and redox properties and varied surface molecular structure. MoO_3 based heterogeneous catalyst has been extensively investigated for its application in industrial catalytic process such as hydro-desulfurization [8], metathesis [9], oxidation and oxidative dehydrogenation reactions [10]. Molybdenum species supported on a variety of oxide support such as ZrO_2, SiO_2, Al_2O_3, TiO_2, CeO_2, CeO_2–ZrO_2 and MCM-41 has been reported in literature [11–20]. The flexibility of the Mo-catalyst to form different molecular structure and the ability of Mo atoms to assume various oxidation states, depending on the pre-treatment and the reaction atmosphere are the main features invoked to explain its catalytic activity. Among the different supported MoO_3 system, the ZrO_2–MoO_3 composite oxides have been extensively investigated for catalytic applications [11–15]. This is due to the superior physicochemical properties exhibited by zirconia such as good thermal stability, extreme

* Corresponding author. Tel.: +916612462651; fax: +91 6612462651.
E-mail address: brajam@nitrkl.ac.in (B.G. Mishra).

1381-1169/$ – see front matter © 2011 Elsevier B.V. All rights reserved.
doi:10.1016/j.molcata.2011.02.017

hardness, stability under reducing conditions, and both surface acidic and basic functions. Although there are investigations on the structure, transformation and application of this important class of composite oxide, there are no reports available dealing with the catalytic activity of these materials synthesized using solution combustion method. Moreover, the catalytic applications studied so far are restricted to industrial catalysis. There is a vast scope to apply this important catalytic material in organic synthesis involving fine chemicals.

The solution combustion method, one of the convenient modifications of self-propagating high temperature synthesis is widely used for material preparation [21]. In past few years, many novel procedures have been adopted during combustion synthesis such as use of organic compounds as fuels, microwave and sonic wave as energy source to obtain materials with desired properties. In solution combustion method, organic compounds containing reducible functional groups are employed as fuels and metal nitrates are used as oxidizers. The exothermic combustion reaction between the fuel and the oxidizer results in the formation of unagglomerated solid particles with simultaneous evolution of large amounts gaseous products [22–25]. The nature and amount of fuel in a reaction mixture can effectively control the particle size and morphology of the combustion products. Nitrogen containing compounds are widely employed as fuel because of their natural tendency to act as chelating ligands forming complexes with the metal ions [22,23]. The specificity of a fuel for synthesis of metal oxides, depends on the metal–ligand complex formation and the thermodynamics of the reaction. Glycine is a bidentate ligand with amphoteric character which can have different mode of bonding with the metal ions. The zwiterionic character of glycine molecule is useful in effectively complexing with metal ions of varying ionic sizes [26]. This in turn helps in preventing their selective precipitation and maintains a compositional homogeneity among the constituents. In this present investigation, we have employed glycine as fuel for the preparation MoO_3–ZrO_2 composite oxide using solution combustion route. Our investigation has lead to the conclusion that that fuel nature and content are crucial factors which affect the physicochemical characteristics of the composite oxide which in turn affect its catalytic activity.

2. Experimental

2.1. Combustion synthesis of MoO_3–ZrO_2 composite oxides

Zirconyl nitrate ($ZrO(NO_3)_2{\cdot}xH_2O$) and glycine were procured from Merck India. Ammonium heptamolybdate was obtained from S.D. Fine chemicals Ltd., India. All the chemicals were used as received without any further purification. Montmorillonite K10 was obtained from Sigma–Aldrich limited, India and used as such for the reactions. Pure ZrO_2 and MoO_3 (10 mol%)-ZrO_2 composite oxide materials were prepared by combustion synthesis using $ZrO(NO_3)_2{\cdot}xH_2O$, ammonium heptamolybdate as salt precursor and glycine as fuel. In a typical preparation procedure, required amounts of zirconyl nitrate, ammonium heptamolybdate and glycine were dissolved in minimum amount of double distilled water and the mixture was kept in a furnace, preheated to 400 °C. The mixture ignited instantaneously producing a foamy material of MO_3–ZrO_2 simultaneously releasing a lot of gaseous products. The fuel to oxidizer ratio (F/O) was calculated by using the method described by Jain et al. [27]. The F/O ratio was varied from 0.5 to 1.5 to study the effect of fuel content on the physicochemical characteristics of the MoO_3–ZrO_2 composite oxide materials. The MoO_3 (10 mol%)-ZrO_2 materials prepared by this method are referred to as 10MoZr-G in the subsequent text. For the sake of comparison, the 10MoZr materials were also prepared using urea and hexamethylene tetraamine as fuels (designated as 10MoZr-U and 10MoZr-H). The 10MoZr catalyst was also prepared by the impregnation of the hydrous zirconia with ammonium heptamolybdate solution (designated as 10MoZr-I). The sulfated zirconia catalyst was synthesized by sulfate treatment of hydrous zirconia material using the procedure described elsewhere [28].

2.2. Characterization techniques

The XRD patterns of the pure ZrO_2 and 10MoZr-G composite oxide materials were recorded using a Philips PAN analytical diffractometer using Ni filtered CuKα_1 (λ = 1.5405 Å) radiation in the range of 20–70° at a scan rate of 2° per minute. The crystallite size has been calculated from the Fourier line shape analysis following the Warren and Averbach method [29]. The UV–visible-absorbance spectra of the samples were recorded using Shimadzu spectrometer model 2450 with $BaSO_4$ coated integration sphere. Scanning electron micrograph (SEM) was taken using JEOL JSM-6480 LV microscope (acceleration voltage 20 kV). The sample powders were deposited on a carbon tape before mounting on a sample holder. Transmission electron micrographs (TEM) of the samples were recorded using PHILIPS CM 200 equipment using carbon coated copper grids. The specific surface area of the combustion synthesized materials was determined by BET method using N_2 adsorption/desorption at 77 K on an AUTOSORB 1 Quantachorme instrument. The number of acid sites in the composite oxide materials was obtained from TG analysis of adsorbed *n*-butyl amine [30]. The oxide samples were exposed to the reagent grade *n*-butyl amine for 48 h in desiccators. Thermogravimetry analysis of the samples was then performed in nitrogen atmosphere from room temperature to 550 °C at a rate of 10 °C min^{-1}. The percentage weight loss corresponding to the temperature range of 200–450 °C were calculated and the acidity was obtained assuming each base molecule interacted with a single acidic site of the oxide material. Melting points were measured using LABTRONICS LT-110 model and are uncorrected. ^{1}H NMR spectra were recorded with Bruker spectrometer at 400 MHz using TMS as internal standard. IR spectra were recorded using Perkin-Elmer IR spectrophotometer as KBr pellets. Reactions were monitored by thin layer chromatography on 0.2 mm silica gel F-254 plates. GC analysis was performed by Nucon 5765 equipment fitted with a FID detector and OV-101 packed column. All the reaction products are known compounds and are identified by comparing their physical and spectral characteristics with the literature reported values.

2.3. Synthesis of octahydroquinazolinones

The synthesis of octahydroquinazolinones was carried out under solvent free condition using microwave as an energy source as well as water as a green reaction media. For reaction under microwave condition a neat mixture of benzaldehyde (1 mmol), dimedone (1 mmol), urea (1.5 mmol) and 100 mg of catalyst (10MoZr-G) was exposed to the microwave radiation for the required amount of time. The reaction mixture was irradiated at 900 W for the specified time with an intermittent cooling interval of 60 s after every 60 s of microwave irradiation. The progress of the reaction was monitored by TLC. After completion of the reaction, the crude product from the reaction mixture was poured in to 25 mL of ice cold water. The ensuing solid product was filtered, dried and then dissolved in hot ethanol. The ethanolic solution was filtered to separate the heterogeneous catalyst and the filtrate was concentrated under reduced pressure to remove the ethanol and recrystallized. The catalyst was regenerated by washing three times with 10 mL portion of ethanol followed by heat treatment at 400 °C for 1 h. For reaction in aqueous media, the same reaction stoichiometry and similar reaction work up condition is used. The reactions

Table 1
Physicochemical characteristics and catalytic activity of various catalysts screened for the synthesis of octahydroquinazolinone under microwave irradiation and solventfree condition.

Catalyst[a]	Surface area (m^2/g)	Acidity (mmol/g)	Yield[b] (%)	Irradiation time (s)	Rate[c] (mmol h^{-1} g^{-1})	Rate[c] (mmol h^{-1} m^{-2})
ZrO_2	50.8	0.21	25	360	30	0.59
SO_4^{2-}/ZrO_2	45.4	0.39	72	360	75	1.65
10MoZr-U	54.5	0.37	62	300	86	1.57
10MoZr-G	49.4	0.45	82	180	170	3.43
10MoZr-H	44.7	0.26	70	210	128	2.86
10MoZr-I	95.0	0.32	75	360	78	0.82
Mont K-10	185.0	0.35	68	360	72	0.39

[a] All composite oxides synthesized by combustion method corresponds to F/O = 1.
[b] Refers to pure and isolated yield.
[c] Calculated with respect to the benzaldehyde conversion in the reaction mixture analyzed using gas chromatography.

were carried out under reflux condition under stirring for the specified time using 5 mL of double distilled water as solvent. All the products obtained are known compounds and are characterized by comparing their IR, ^{1}H NMR and melting points with those reported in literature [1–7].

2.4. Physical and spectral data of some selected compounds

7,7-Dimethyl-4-phenyl-4,6,7,8-tetrahydro-1H,3H-quinazoline-2,5-dione (Table 2, entry 1)*:* Mp: 291–292 °C, IR (KBr): 3325 (br), 3262 (br), 2963 (br), 1710 (s), 1670 (s),1605 (vs), 1442 (w), 1374 (s), 1228 (s), 764 (s), 689(w), 484(w) cm^{-1}, ^{1}H NMR (400 MHz, $CDCl_3$): δ 0.92 (s, 3H, CH_3); 1.06 (s, 3H, CH_3); 2.15 (q, 2H,CH_2); 2.35 (q, 2H, CH_2); 5.25 (d, 1H, CH); 7.35–7.20 (m, 5H, Ar); 7.49 (s, 1H, NH); 9.42 (s,1H, NH).

4-(2-Chloro-phenyl)-7,7-dimethyl-4,6,7,8-tetrahydro-1H,3H-quinazoline-2,5-dione (Table 2, entry 2)*:* Mp: 281–282 °C, IR (KBr): 3350 (br), 3250 (br), 2962 (br), 1710(s), 1670 (s), 1612 (vs), 1452 (s), 1371 (s), 1223 (s), 755 (s), 566 (w), 476 (w), ^{1}H NMR (400 MHz, $CDCl_3$ + DMSO-d_6): δ 0.98 (3H, s, CH_3); 1.05 (3H, s, CH_3); 2.10 (2H, q, CH_2); 2.42 (2H, q, CH_2); 5.52 (1H, d, CH); 7.25–7.42 (4H, m, Ar); 7.72 (1H, d, NH); 9.50 (1H, s, NH).

7,7-Dimethyl-4-phenyl-2-thioxo-2,3,4,6,7,8-hexahydro-1H-quinazolin-5-one (Table 2, entry 10)*:* Mp: 284–286 °C, IR (KBr): 3255 (br), 3172 (br), 2962 (br), 1623 (vs), 1562 (s), 1452 (s), 1370 (s), 1142 (m), 1095 (sh), 1055 (w), 695 (w), 516 (w), 427 (w) cm^{-1}, ^{1}HNMR (400 MHz, $CDCl_3$ + DMSO-d_6): δ 0.96(s, 3H, CH_3); 1.10 (s, 3H, CH_3); 2.24 (q, 2H, CH_2); 2.35(s, 2H, CH_2); 5.28 (d, 1H, CH); 7.38–7.26 (m, 5H, Ar); 9.51(s, 1H, NH); 10.32(s, 1H, NH).

3. Results and discussion

3.1. Characterization of the MoO_3–ZrO_2 composite oxides

Fig. 1 shows the X-ray diffraction patterns of the ZrO_2 and 10MoZr-G catalyst prepared by solution combustion method using glycine as fuel. The pure ZrO_2 shows intense and broad diffraction peaks at 2θ values of 30.2°, 34.9°, 50.4° and 60.3° corresponding to the presence of tetragonal phase of zirconia. The characteristics reflections from the monoclinic phase is absent in the XRD profile of combustion synthesized zirconia sample. This observation clearly suggests the selective stabilization of the metastable tetragonal phase of zirconia in combustion synthesis process. Addition of 10 mol% MoO_3 into the zirconia matrix does not result in any significant change in the XRD profile of zirconia. No XRD peaks corresponding to the presence of separate crystalline phase of MoO_3 was observed in the XRD patterns of the composite oxide samples. The 10MoZr-G material show broad but intense reflections. The XRD peak intensity was found to increase with increase in the fuel content in the combustion mixture. Simultaneously, two new peaks were observed at 2θ values of 27.5° and 32.5°. These peaks corresponds to the presence of a small amount of $Zr(MoO_4)_2$ spinel phase (JCPDS file No. 39-1438). The intensity of the spinel $Zr(MoO_4)_2$ peak was found to increase with increase in F/O ratio. The crystallite size were calculated from the Fourier line shape analysis for all the combustion synthesized samples following the Warren and Averbach method [29] using software BRAEDTH, the details of which are available in literature [31]. The peak position (2θ), full width at half maximum (FWHM) and intensity was calculated using commercially available soft ware (PEAK FIT) for each peak of the XRD data. The indexing of the peaks was carried out using 2θ and intensity value of each peak using standard computer software POWD [32]. The best agreement between the observed and the calculated interplaner spacing and Bragg angles was found for tetragonal crystal structure. The calculated volume-weighted distributions, (*PV*), and crystallite size as function of the Fourier length (*L*) for the ZrO_2 and 10MoZr samples is given in Fig. 2a and b, respectively. The wide distribution function observed for the 10MoZr-G (F/O = 1.5) sample indicates that the particles are polycrystalline with larger parti-

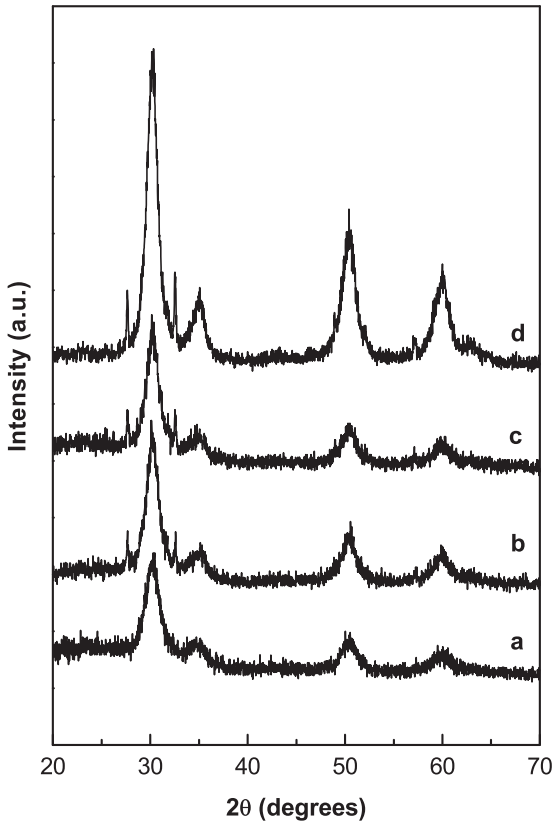

Fig. 1. X-ray diffraction patterns of (a) ZrO_2, (b) 10MoZr-G (F/O = 0.5) (c) 10MoZr-G (F/O = 1) and (d) 10MoZr-G (F/O = 1.5).

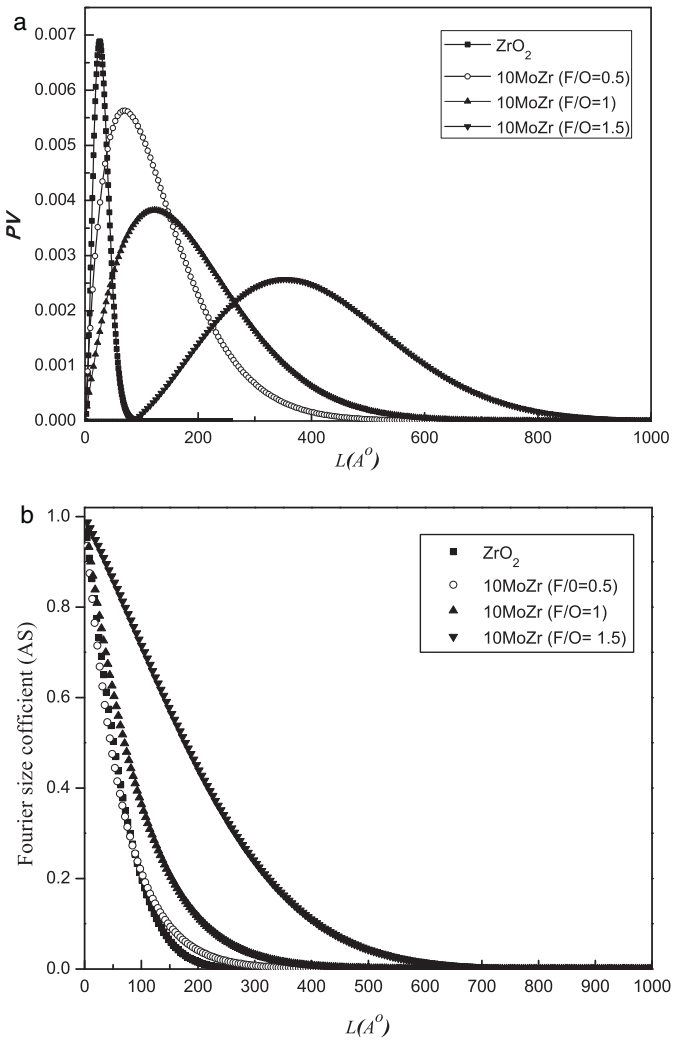

Fig. 2. Fourier line profile analysis plots for the ZrO_2 and 10MoZr-G samples.

cle size. The pure ZrO_2 and 10MoZr-G (F/O = 0.5) material show a comparable narrower size distribution function as compared to the 10MoZr-G (F/O = 1.0) and 10MoZr-G (F/O = 1.5) material (Fig. 2a). The crystallite sizes of the ZrO_2, 10MoZr-G (F/O = 0.5), 10MoZr-G (F/O = 1.0) and 10MoZr-G (F/O = 1.5) materials were calculated to be 9, 7, 11 and 39 nm, respectively (Fig. 2b).

The UV–vis spectra of the combustion synthesized ZrO_2 and 10MoZr-G materials are presented in Fig. 3. The combustion synthesized ZrO_2 prepared using glycine as fuel shows a prominent absorption band at 210 nm with absorption edge around 260 nm (Fig. 3a). Zirconia is an insulator material which shows interband transition in the UV region of the electronic spectrum corresponding to the $O^{2-}(2p) \rightarrow Zr^{4+}$ (4d) transition. Among the polymorphic forms of zirconia, the octacoordinated tetragonal (space group $Fm3m$) and cubic (space group $P4_2/nmc$) phases shows UV absorption maxima in the range of 200–210 nm where as the heptacoordinated monoclinic phase (space group $P2_1/c$) shows maxima around 240 nm [33]. It has been observed that as the coordination number of Zr^{4+} ion decreases from 8 to 6, the LMCT absorption maxima progressively shifts to lower energy (higher wavelength) [34,35]. The prominent absorption band observed for pure zirconia at peak maxima of 210 nm can be assigned to the $O^{2-} \rightarrow Zr^{4+}$ charge transfer transition arising out of the tetragonal phase of zirconia. This observation is complementary to the XRD result where stabilization of tetragonal phase was observed. Pure MoO_3 shows two well defined absorption bands at 240 and 320 nm (Fig. 3e). Since Mo^{6+} has a d^0 electronic configuration, the only absorption feature expected is due to the ligand–metal charge transfer transition (LMCT), $O^{2-} \rightarrow Mo^{6+}$ which occur in the range of 200–400 nm. Depending on the coordination preference and local symmetry, Mo (VI) ions show different absorption bands in the electronic spectrum. The peak at 240 nm for pure MoO_3 has been assigned to the isolated MoO_4 species with tetrahedral symmetry where as the peak at 320 nm has been assigned to bulk polymolybdate species [36–38]. The addition of MoO_3 to zirconia matrix significantly modifies the absorption spectra of the combustion synthesized MoO_3–ZrO_2 composite oxide. The 10MoZr-G samples with different F/O ratio show a prominent band between 220 and 240 nm with the absorption edge extending upto 400 nm. The absorption band at 220–240 nm can be ascribed to the presence of isolated tetrahedral molybdate species with structural distortion. Earlier studies on the UV–vis spectra of dispersed MoO_3 system have revealed three absorption regions corresponding to the presence of isolated molybdate species (220–250 nm), polymolybdate clusters (260–290 nm) and bulk type molybdate (>315 nm) [36–38]. Considering the asymmetric nature of the spectra for the 10MoZr-G materials it is likely that polymolybdate species such as hepta and octamolybdate clusters can exist on the zirconia surface (Fig. 3b–d). However, it is certain from the UV Vis study that the molybdate species exist in a highly dispersed from in the composite oxide and there is no indication of the presence of bulk type molybdate. The peak at 320 nm corresponding to the bulk type MoO_3 was absent for 10MoZr-G composite oxides. There is no apparent change in the absorption feature when the F/O ratio was varied between 0.5 and 1.5 indicating the presence of identical molybdate species in these samples.

The scanning electron micrograph of the ZrO_2 and 10MoZr-G material prepared using different F/O ratio is presented in Fig. 4. The pure zirconia prepared using glycine as fuel shows well ordered particle morphology. This can be ascribed to the effective com-

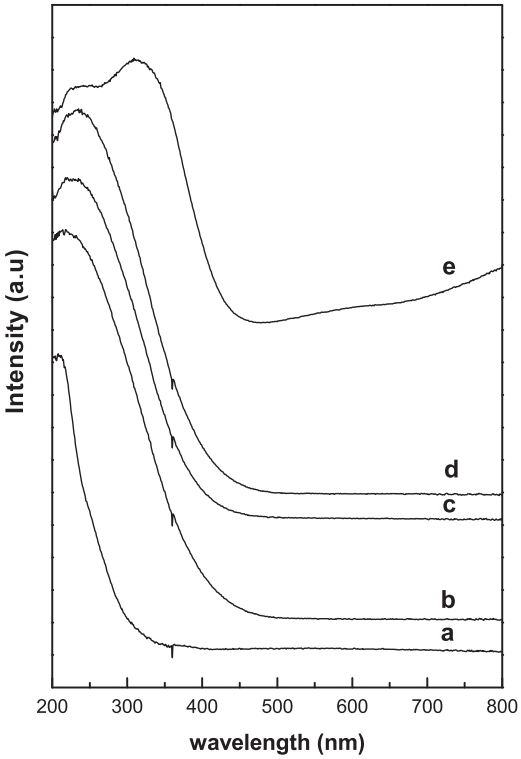

Fig. 3. UV–vis spectra of (a) ZrO_2, (b) 10MoZr-G (F/O = 0.5), (c) 10MoZr-G (F/O = 1) (d) 10MoZr-G (F/O = 1.5) and (e) pure MoO_3 materials.

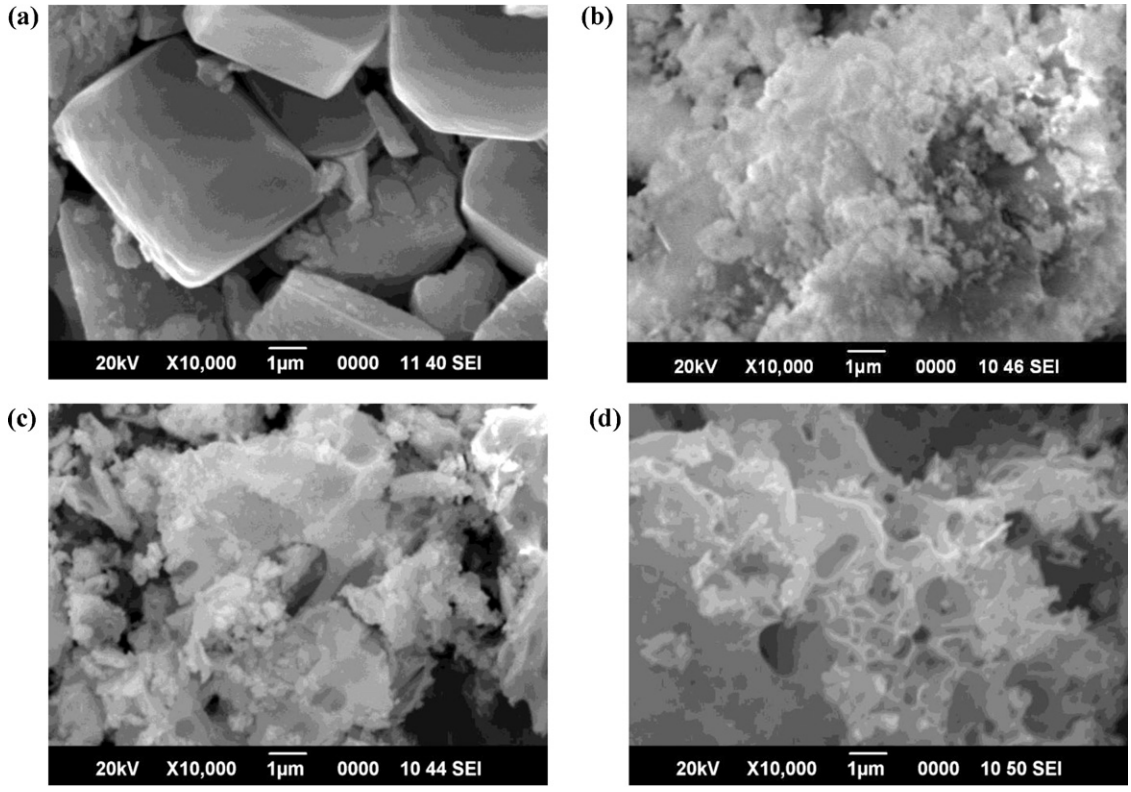

Fig. 4. Scanning Electron micrograph of (a) ZrO_2, (b) 10MoZr-G (F/O = 0.5), (c) 10MoZr-G (F/O = 1) and (d) 10MoZr-G (F/O = 1.5) materials.

plexation and prevention of hydrolysis of the Zr^{4+} ions in the combustion mixture. Zirconium ions being acidic in nature can undergo considerable hydrolysis in the combustion mixture in presence of nitrogen containing fuels. The uncontrolled hydrolysis of the Zr^{4+} ions and subsequent combustion can lead to particles with random morphology and sizes. The zwiterionic character of glycine molecule is useful in effectively complexing with Zr^{4+} ions which prevent hydrolysis of ions and maintains a compositional homogeneity in the combustion mixture. The 10MoZr-G materials prepared using glycine fuel are of low density and spongy in nature. The particles are found to be agglomerated and of irregular shape and size. With increase in F/O ratio the spongy nature was found to increase. Numerous macropores and intraparticle pores are observed for the 10MoZr-G samples. The presence of the macropores can be ascribed to the evolution of large amount of gaseous products during the combustion process. Theoretically, for the formation of one mole of 10MoZr-G, 6.69, 6.94 and 7.21 moles of gases are generated for F/O ratio of 0.5, 1 and 1.5, respectively. The higher amount of gases generated leaves the material porous and spongy.

The transmission electron micrographs of ZrO_2 and 10MoZr-G (F/O = 1) materials are shown in Fig. 5. The TEM image of pure zirconia shows the presence of uniform nanoparticles with size in the range of 5–10 nm. Similarly, for the 10MoZr-G material, nanoparticles with size in the range of 10–20 nm were observed in the TEM study. The Fourier line shape analysis data was found to corroborate the TEM results. The 10MoZr-U and 10MoZr-H materials synthesized using urea and hexamethylene tetraamine show particles with size in the range of 20–30 nm whereas the 10MoZr-I materials show larger particles with size in the range of 50–100 nm (Fig. 5). The TEM observations indicate that combustion synthesis is quite effective in the preparation of nanosize particles. During combustion synthesis process, the reactants are uniformly dispersed at molecular level in the combustion mixture. When combustion occurs, the nucleation and growth of the particles take place only through the short-distance diffusion of the nearby atoms. Due to the shorter life span of the combustion reaction, the long-distance diffusion of the atoms is not facilitated resulting in the formation of nanosized materials.

3.2. Catalytic studies for synthesis of octahydroquinazolinones

The catalytic activity of 10MoZr-G (F/O = 1) catalyst was evaluated for the synthesis of octahydroquinazolinones by one pot multi-component condensation of dimedone, aromatic aldehydes and urea (Scheme 1). Catalysts having different active sites and acidic strength were initially screened for the synthesis of octahydroquinazolinone under solvent free condition using microwave as an energy source. Table 1 shows the physicochemical characteristics and catalytic activity of several zirconia based catalysts screened for the condensation of benzaldehyde, dimedone and urea. For the sake of comparison, the 10MoZr material was prepared by combustion route using urea (10MoZr-U) and hexamethylene tetraamine (10MoZr-H) as fuels at F/O = 1. The 10MoZr material was also prepared by impregnation of ammonium heptamolyb-

Table 2
10MoZr-G (F/O = 1) catalyzed synthesis of octahydroqunazolinines under solvent-free condition and microwave irradiation.

Entry	*R*	*X*	Time (s)	Yield (%)
1	H	O	180	82
2	2-Cl	O	180	86
3	4-Cl	O	150	89
4	2-NO_2	O	200	82
5	3-NO_2	O	180	86
6	4-NO_2	O	180	88
7	4-OMe	O	240	79
8	2-OH	O	240	75
9	4-OH	O	220	81
10	H	S	270	74
11	4-OH	S	300	63
12	4-Cl	S	250	81

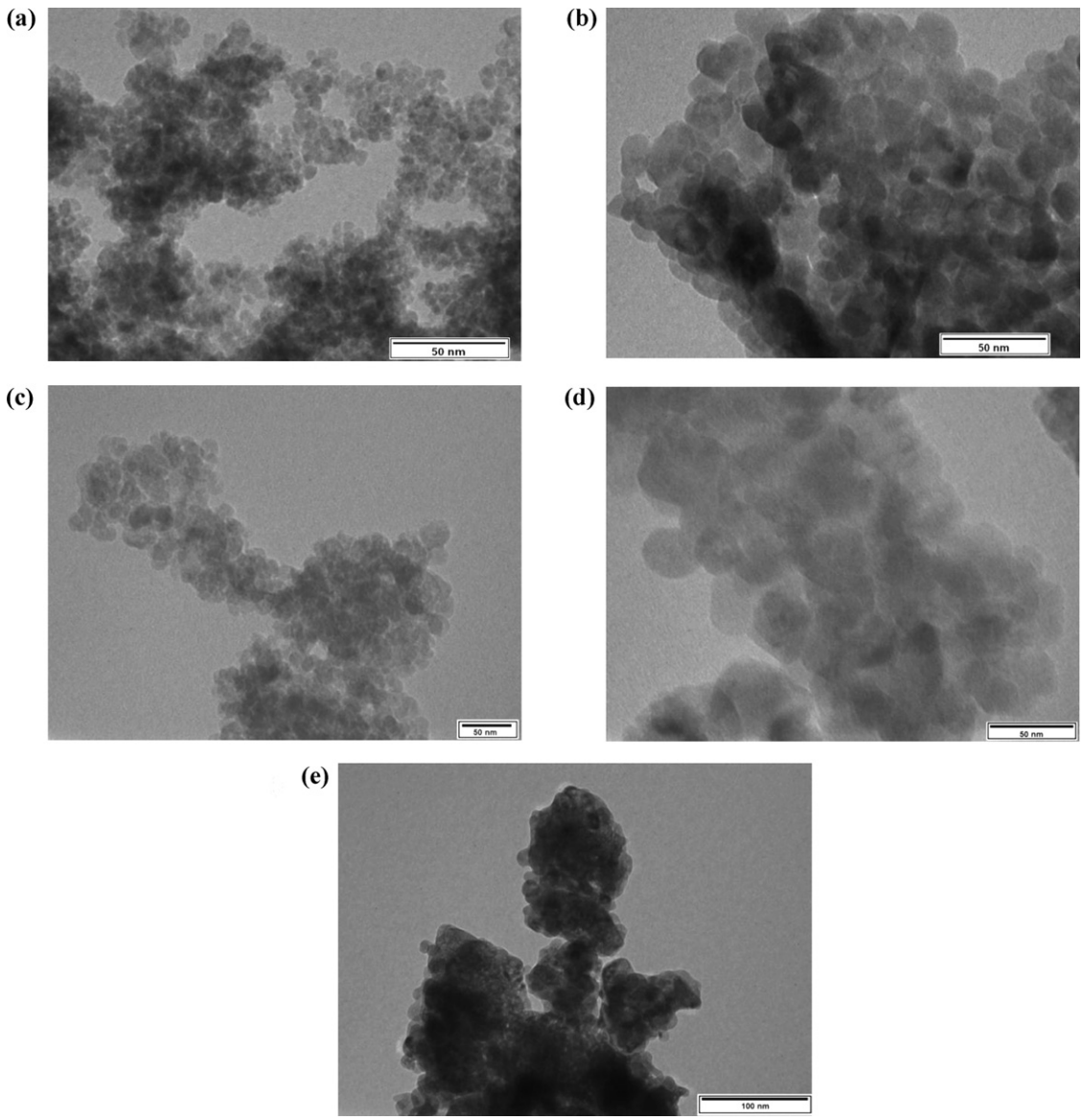

Fig. 5. Transmission electron micrographs of (a) ZrO_2 and (b) 10MoZr-G (F/O = 1), (c) 10MoZr-U (F/O = 1), (d)10MoZr-H (F/O = 1) and (e) 10MoZr-I.

date to hydrous zirconia powder prepared by precipitation method using ammonia as precipitating agent (10MoZr-I). Under identical reaction conditions, the 10MoZr-G (F/O = 1) material was found to be most efficient giving 82% yield of the product in a minimum irradiation time of 180 s. 10MoZr-I and sulfated zirconia also show comparable yield however they require considerably longer irradiation time. Among all the catalyst the 10MoZr-G (F/O = 1) material display more number of acidic sites compared to other catalytic materials used (Table 1). Since the catalysts screened show different surface area and acidity, the reaction rate were

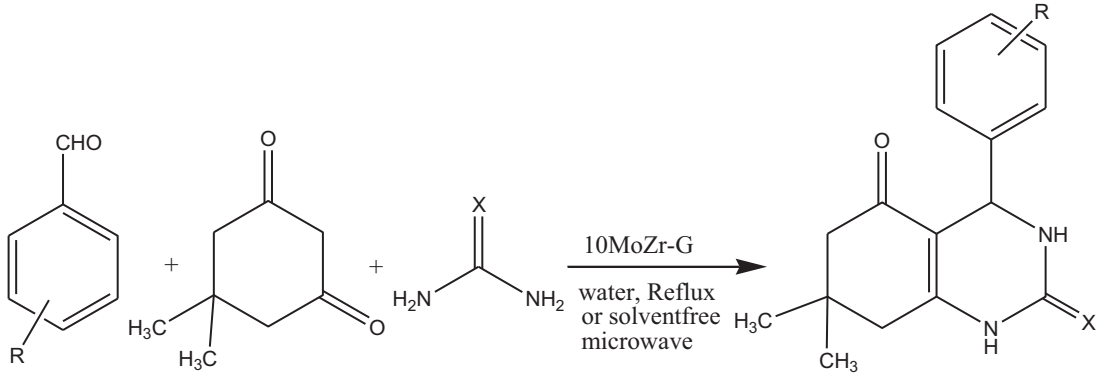

Scheme 1. One pot synthesis of octahydroquinazolinones using 10MoZr-G catalyst.

Table 3
10MoZr-G (F/O = 1) catalyzed synthesis of octahydroqunazolinines in aqueous media.

Entry	*R*	*X*	Time (h)	Yield (%)
1	H	O	6	74
2	2-Cl	O	5	78
3	4-Cl	O	4	82
4	2-NO_2	O	5	72
5	3-NO_2	O	6	76
6	4-NO_2	O	5	80
7	4-OMe	O	10	66
8	2-OH	O	10	70
9	4-OH	O	10	68
10	H	S	8	68
11	4-OH	S	10	62
12	4-Cl	S	8	75

calculated in terms of unit surface area and acidic sites by estimating the benzaldehyde conversion in the reaction mixture by GC analysis. It was observed that the 10MoZr-G (F/O = 1) catalyst shows higher reaction rates as compared to other materials. Based on the results described in the Table 1, the 10MoZr-G (F/O = 1) catalyst was selected for further studies. The reaction parameters were optimized by varying catalyst amount and reaction stoichiometry. It was observed that the for a reaction involving 1 mmol of the reactants, 100 mg of the catalyst is ideal for an efficient condensation of the reactants under solvent free condition using microwave as an energy source. The optimum reactant ratio was found to be 1:1:1.5 for benzaldehyde, dimedone and urea or thiourea, respectively. Ensuing optimized conditions for this multicomponent reaction, we explored the scope and limitations of this reaction using different substituted aromatic aldehydes and urea or thiourea (Table 2). It was observed that the aromatic aldehydes having electron-withdrawing groups react faster in the optimized protocol as compared to the aldehydes having electron donating groups. Unlike those of urea, the reaction of thiourea proceeded at lower rate to give octahydroquinazolinones (Table 2). The 10MoZr-G (F/O = 1) catalyst was further explored for the synthesis of octahydroquinazolinones in aqueous media. For reactions in water, the multicomponent condensation was carried out under reflux conditions using 5 ml of the solvent using the optimized reaction stoichiometry and catalyst amount of 100 mg. Table 3 shows the results of the catalytic studies carried out in aqueous media using 10MoZr-G (F/O = 1) catalyst. It was observed that the catalyst was quite efficient for the one pot synthesis giving good yield of the products in a time span of 5–12 h. A variety of aldehydes containing electron withdrawing and releasing groups reacted efficiently to give the corresponding octahydroquinazolinones in good yield and purity. Comparing both protocols, although the yields of the products are comparable, the reaction rate is quite sluggish in aqueous media as compared to the microwave assisted synthesis under solvent free condition. The recyclability of the catalyst was evaluated in the aqueous media. The catalyst was regenerated by washing with 10 mL ethanol followed by heat treatment at 400 °C for 1 h. The regenerated catalyst was used for three consecutive cycles without any significant loss in catalytic activity (Table 3, entry1, 74%, 1st, 70% 2nd, 67%, 3rd).

4. Conclusion

In the present investigation we have synthesized MoO_3–ZrO_2 nanocomposite oxide by solution combustion method. The selective stabilization of the tetragonal phase of zirconia was observed in the composite oxide. The particle size of the composite oxide calculated from Fourier line shape analysis of the XRD profiles as well as TEM. The particle size was found to be in the range of 5–40 nm depending upon the amount of fuel used. The molybdina component was found to be present in a highly dispersed state in the form of isolated tetrahedral and polymolybdate clusters in the composite oxide material. SEM study of the composite oxide indicate the material to be of low density and spongy in nature. The combustion synthesized 10MoZr-G composite oxide was explored for a rapid, convenient and environmentally benign synthesis of biologically important octahydroquinazolinones under solvent-free conditions and in aqueous medium. The combustion synthesized 10MoZr-G catalyst was highly active for the multicomponent reactions generating a variety of structurally diverse octahydroquinazolinones with good yield and purity of the products. The protocol developed using the MoO_3–ZrO_2 catalyst was found to be advantageous in terms of simple experimentation, preclusion of toxic solvents, recyclable catalyst and high yield and purity of the synthesized compounds.

Acknowledgement

The authors would like to thank Council of Scientific and Industrial Research (CSIR), New Delhi for financial support.

References

[1] M. Kidwai, S. Saxena, M.K.R. Khan, S.S. Thukral, Eur. J. Med. Chem. 40 (2005) 816–819.
[2] M. Yarim, S. Sarac, F.S. Kilic, K. Erol, Il Farmaco 58 (2003) 17–24.
[3] J.M. Khurana, S. Kumar, Monatsh Chem. 141 (2010) 561–564.
[4] H. Lin, Q. Zhao, B. Xu, X. Wang, J. Mol. Catal. A 268 (2007) 221–226.
[5] Z. Hassani, M.R. Islami, M. Kalantari Bioorg, Med. Chem. Lett. 16 (2006) 4479.
[6] S. Kantevari, R. Bantu, L. Nagarapu, ARKIVOC xvi (2006) 136–148.
[7] K.S. Niralwad, B.B. Shingate, M.S. Shingare, Tetrahedron Lett. 51 (2010) 3616–3618.
[8] P. Grange, Catal. Rev. Sci. Eng. 21 (1980) 135–181.
[9] W. Grunert, A.Y. Stakheev, W. Morke, J. Catal. 135 (1992) 269–286.
[10] M.A. Banares, J.L.G. Fierro, J.B. Moffat, J. Catal. 142 (1993) 406–417.
[11] E.A. El-Sharkawy, A.S. Khder, A.I. Ahmed, Micropor. Mesopor. Mater. 102 (2007) 128–137.
[12] K.V.R. Chary, K.R. Reddy, G. Kishan, J.W. Niemantsverdriet, G. Mestl, J. Catal. 226 (2004) 283–291.
[13] J.C. Yori, C.L. Pieck, J.M. Parera, Catal. Lett. 64 (2000) 141–146.
[14] H. Wan, D. Li, H. Zhu, Y. Zhang, L. Dong, Y. Hu, B. Liu, K. Sun, L. Dong, Y. Chen, J. Colloid Interface Sci. 326 (2008) 28–34.
[15] A.S.C. Brown, J.S.J. Hargreaves, S.H. Taylor, Catal. Lett. 57 (1999) 109–113.
[16] F. Chen, H. Ma, B. Wang, Chem. Eng. J. 141 (2008) 375–378.
[17] S.H. Elder, F.M. Cot, Y. Su, S.M. Heald, A.M. Tyryshkin, M.K. Bowman, Y. Gao, A.G. Joly, M.L. Balmer, A.C. Kolwaite, K.A. Magrini, D.M. Blake, J. Am. Chem. Soc. 122 (2000) 5138–5146.
[18] J. Kaur, V.D. Vankar, M.C. Bhatnagar, Sens. Actuators B 133 (2008) 650–655.
[19] V.S. Escribano, J.M.G. Amores, E.F. López, C.H. Martínez, G. Busca, C. Resini, Mater. Chem. Phys. 114 (2009) 848–853.
[20] Z. Li, B. Cheng, K. Su, Y. Gu, P. Xi, M. Guo, J. Mol. Catal. A 289 (2008) 100–105.
[21] C.N.R. Rao, Chemical Approches to the Synthesis of Inorganic Materials, Wiley Eastern Limited, New Delhi, 1994.
[22] K.C. Patil, M.S. Hegde, T. Rattan, S.T. Aruna, Chemistry of Nanocrystalline Oxide Materials, World Scientific Publishing Co. Pte. Ltd., 2008.
[23] K.C. Patil, S.T. Aruna, T. Mimani, Curr. Opin. Solid State Mater. Sci. 6 (2002) 507–512.
[24] G.R. Rao, B.G. Mishra, H.R. Sahu, Mater. Lett. 58 (2004) 3523–3527.
[25] M.A. Naik, B.G. Mishra, A. Dubey, Colloids Surf. A 317 (2008) 234–238.
[26] J. Kishan, V. Mangam, B.S.B. Reddy, S. Das, K. Das, J. Alloys Compd. 490 (2010) 631–636.
[27] S.R. Jain, K.C. Adiga, V.R. Verneker, Combust. Flame 40 (1981) 71–79.
[28] D. Kumar, B.G. Mishra, M.S. Swapna, Chem. Lett. 35 (2006) 1074–1075.
[29] B.E. Warren, B.L. Averbach, J. Appl. Phys. 21 (1950) 595–599.
[30] C. Breen, Clay Miner. 26 (1991) 487–496.
[31] D. Balzar, H. Ledbetter, J. Appl. Crystallogr. 26 (1993) 97–103.
[32] "POWD", An interactive powder diffraction data interpretation and indexing programme, ver. 2.1 E. Wu, School of physical science, Flinder Univ. of South Australia, BedfordPark, S. A 5042, Australia.
[33] E.F. Loïpez, V.S. Escribano, M. Panizza, M.M. Carnascialic, G. Busca, J. Mater. Chem. 11 (2001) 1891–1897.
[34] M. Scheithauer, R.K. Grasselli, H. Knozinger, Langmuir 14 (1998) 3019–3029.
[35] M. Li, Z. Feng, G. Xiong, P. Ying, Q. Xin, C. Li, J. Phys. Chem. B 105 (2001) 8107–8111.
[36] M. Henker, K.P. Wendlandt, J. Valyon, Appl. Catal. A 69 (1991) 205–220.
[37] M.M. Mohamed, S.M.A. Katib, Appl. Catal. A 287 (2005) 236–243.
[38] Z. Liu, Y. Chen, J. Catal. 177 (1998) 314–324.